Collins Katrina (Orcid ID: 0000-0002-9603-6731)
Antic Tatjana (Orcid ID: 0000-0002-0455-9413)
Argani Pedram (Orcid ID: 0000-0001-8797-9474)
Mehra Rohit (Orcid ID: 0000-0002-6955-8884)
Williamson Sean R (Orcid ID: 0000-0002-3898-1460)
Idrees Muhammad T (Orcid ID: 0000-0001-6611-6389)
Anderson William (Orcid ID: 0000-0002-5807-7831)
Hornick Jason L (Orcid ID: 0000-0001-6475-8345)
Acosta Andres M. (Orcid ID: 0000-0001-8817-6331)

Merlin Immunohistochemistry Is Useful in Diagnosis of Tumors within the Spectrum of Biphasic Hyalinizing Psammomatous Renal Cell Carcinoma

Authors:
Katrina Collins, MD[1#], Michael Hwang, MD[1#], Tatjana Antic, MD[2], Ajit Paintal, MD[3], Pedram Argani, MD[4], Andres Matoso, MD[4], Arun Gopinath, MD[5], Brett Baskovich, MD[5], Rohit Mehra, MD[6], Sean R. Williamson, MD[7], Muhammad T. Idrees[1], MD, Justine A. Barletta, MD[8], William J. Anderson MBChB[8], MD, Michelle S. Hirsch, MD, PhD[8], Jason L. Hornick, MD, PhD[8], Andres M. Acosta, MD[8*]

From the Department of Pathology of:
[1] Indiana University School of Medicine, Indianapolis, IN, USA.
[2] The University of Chicago, Chicago, IL, USA
[3] NorthShore University HealthSystem, Evanston, IL, USA
[4] Johns Hopkins University School of Medicine, Baltimore, MD, USA
[5] University of Florida College of Medicine Jacksonville, Jacksonville, FL, USA
[6] Michigan Medicine and University of Michigan, Ann Arbor, MI, USA
[7] Cleveland Clinic, Cleveland, OH, USA
[8] Brigham and Women's Hospital/Harvard Medical School, Boston, MA, USA

[#]These authors contributed equally to the study.

Running title: Merlin expression in BHP RCC

Keywords: renal neoplasm, NF2, merlin, mutation, renal cell carcinoma,

***Corresponding author:**
Andrés M. Acosta, MD
Department of Pathology, Brigham and Women's Hospital
75 Francis Street, Boston, MA 02115 USA
Tel: 617-525-8186
Fax: 617-264-5118
Email: aacosta4@bwh.harvard.edu

This is the author manuscript accepted for publication and has undergone full peer review but has not been through the copyediting, typesetting, pagination and proofreading process, which may lead to differences between this version and the Version of Record. Please cite this article as doi: 10.1111/his.14731

Conflicts of Interest Statement
The authors declare that they have no conflicts of interest.

Data availability Statement
The data generated in this study are available from the corresponding author upon reasonable request.

Abstract

Biphasic hyalinizing psammomatous (BHP) renal cell carcinoma (RCC) is a newly described entity, currently a proposed/emerging entity within the spectrum of papillary renal cell carcinoma in the WHO 2022 classification. Molecular analyses have discovered that BHP RCC consistently harbor somatic mutations in the neurofibromin 2 *(NF2)* gene. The *NF2* gene product, merlin, is known to primarily function as a tumor suppressor. Merlin protein loss correlates closely with the presence of *NF2* mutations in benign and malignant tumors arising in different sites. In the present study, we explored the role of merlin immunohistochemistry (IHC) in tumors within the spectrum of BHP RCC to determine the diagnostic utility of this marker.

We performed merlin IHC in 13 BHP RCC tumors, 18 papillary RCC tumors, 10 *TFE3*-translocation RCC and 15 cases of *TFEB*-altered RCC (including 13 *TFEB*-rearranged and 2 *TFEB*-amplified). Unequivocal loss of merlin expression in >90% of the tumor cells was observed in 12/13 BHP-RCC (92%), with the remaining tumor demonstrating weak focal cytoplasmic expression in ~10% of the tumor. In contrast, merlin was diffusely or multifocally expressed in all the tumors of the comparator group. In this study, merlin IHC was ~92% sensitive and ~94% specific for BHP RCC. These data suggest that merlin immunohistochemistry is a reliable surrogate marker for the presence of underlying *NF2* gene inactivation, being diagnostically useful to identify BHP RCC.

Introduction

Biphasic hyalinizing psammomatous (BHP) renal cell carcinoma (RCC) is a recently described entity, currently a proposed/emerging entity within the spectrum of papillary renal cell carcinoma in the WHO 2022 classification, characterized by somewhat distinctive morphologic features and recurrent pathogenic *NF2* gene variants. *NF2*, located on 22q12.2, and a member of the Hippo pathway, codes for a protein called merlin (Moesin-Ezrin-Radixin-Like Protein) that functions as a tumor suppressor (1). Merlin protein loss correlates closely with the presence of inactivating mutations in *NF2* in both benign tumors, such as schwannoma and meningioma, as well as malignant tumors, including mesothelioma, breast and prostate cancer, glioma, clear cell renal cell carcinoma, renal cell carcinoma, unclassified, and melanoma. (1-4) Hippo pathway mutations, including those in NF2, are also enriched in other renal tumor subtypes including the mucinous tubular and spindle cell carcinoma of the kidney (5) and sarcomatoid renal cell carcinoma. (6)

The first description of BHP RCC, published by Argani et al. in 2020 (7), included eight tumors with relatively homogeneous morphologic features, including the presence of a biphasic population of neoplastic cells, hyalinized nodules of basement membrane material, and psammomatous calcifications. These authors noted that *NF2* mutations are not specific for BHP RCC as they may be seen as secondary events in other established RCC types (such as clear cell and papillary RCC) as well as in mucinous tubular and spindle cell carcinoma (MTSCC), so the spectrum of these neoplasms remains to be determined. Subsequent studies of renal tumors purportedly driven by

NF2 inactivation have suggested that the morphologic spectrum of this entity may be somewhat wider than initially thought. (8,9) In a study by Wang et al (9), diagnostic utility of merlin IHC was suggested for identification of BHP RCC; however, its diagnostic utility has not yet been systemically investigated and identification of these tumors has relied on high-complexity massively parallel sequencing assays. In this study, we evaluated the utility of merlin immunohistochemistry (IHC) in tumors within the spectrum of BHP RCC, including reported tumors in the original descriptions of this entity. (7-10)

Material and Methods

This retrospective study was performed with the approval of the Institutional Review Boards of Indiana University, Brigham and Women's Hospital (MGB Insight 4.0) and the remaining institutions (when applicable).

Selection of specimens

Tumors within the spectrum of RCC purportedly driven by *NF2* inactivation described in prior studies (henceforth referred to as 'BHP RCC') (7-10) were retrieved from the personal files of the authors, including tumors previously reported by Argani et al., Paintal et al., and Gopinath et al., (7-8,10) as well as newly identified tumors. Additionally, pathology databases and personal consultation files were queried for tumors diagnosed as papillary RCC, *TFE3*-rearranged RCC, *TFEB*-altered RCC (*TFEB*-rearranged RCC and *TFEB*-amplified RCC), and MTSCC (*NF2* mutation status

unknown) with archival formalin-fixed paraffin-embedded (FFPE) tissue available for IHC.

Tumors were initially reviewed by the submitting pathologists, and selected slides were re-reviewed at Indiana University (K.C. and M.H.) and/or Brigham and Women's Hospital (A.M.A.). Clinicopathologic and molecular data were obtained from pathology reports and summaries provided by the authors.

Immunohistochemistry

IHC was performed on 5 µm-thick FFPE tissue sections. Endogenous peroxidase activity was blocked by incubation in hydrogen peroxide (~30 min), and heat-induced antigen retrieval was performed in a pressure cooker with citrate buffer. Staining was performed using an anti-Merlin primary antibody (clone D1D8, rabbit monoclonal, Cell Signaling Technology, Danvers, MA; dilution: 1:200). The Novolink Polymer Detection System (Leica, Buffalo Grove, IL, USA) was used for signal detection. Molecularly characterized mesotheliomas with homozygous *NF2* deletions and wild-type *NF2* were used as positive and negative controls, respectively.

Merlin IHC was assessed by three pathologists (K.C., M.H., A.M.A.). Positive merlin staining was defined as more than 10% tumor cells showing membranous and/or cytoplasmic and nuclear staining of at least moderate intensity. Loss of expression was defined as complete absence of merlin staining. Focal expression (i.e., <10% of tumor cells) was considered inconclusive/equivocal.

Flourescence in situ hybridization

The diagnosis of all *TFE3*-rearranged RCC and *TFEB*-altered RCC was confirmed with fluorescence in-situ hybridization (FISH). Clinically validated FISH studies for *TFEB3* and *TFEB* rearrangements were performed at the University of Michigan, Cleveland Clinic, Johns Hopkins Hospital and Indiana University according to each institution's standard laboratory procedures.

DNA sequencing

Testing for *NF2* was assessed using the solid tumor panels by the University of Chicago, Memorial Sloan Kettering Cancer Center, UT Southwestern, University of Florida Health Jacksonville Molecular Pathology Laboratory and Nanjing Geneseeq Technology Inc. (Nanjing, China) as described in the corresponding publications. (7-10)

Results

Clinicopathologic features of the study tumors

The series included 13 BHP RCC, including 11 cases (85%) with known biallelic loss of *NF2*, as demonstrated by next generation sequencing in prior series (patients 1-11, all published in prior studies) (7-8,10), 1 tumor (8%) with monosomy 22 detected by single nucleotide polymorphism array (case #12), and 1 case (8%) with fitting morphology but no molecular studies available (case #13). All patients were adults, with a median age of 59 years (range 43 to 88 years) and a M:F ratio of 11:2 (**Table 1**). Median tumor size was 3.5 cm (range 1.0 to 7.5 cm) and pathologic stages for resection specimens were: pT1 (8 tumors), pT2 (1 tumor), and pT3a (2 tumors). All tumors demonstrated histologic

features described in previous reports of this entity. (7-10) The majority of tumors reported in earlier studies were well circumscribed but unencapsulated with papillary or tubulopapillary architecture, usually exhibiting a solid pattern of growth. All tumors had a characteristic biphasic appearance composed of large, clear to eosinophilic cells with glomeruloid formations and clusters of small tumor cells with scant cytoplasm and condensed chromatin occasionally in a tubular arrangement around hyaline material. Scattered psammomatous microcalcifications were frequent. (**Figure 1**) (7-8) The comparator group included 18 papillary RCC, 10 *TFE3*-rearranged RCC, 15 *TFEB*-altered RCC (13 *TFEB*-rearranged and 2 *TFEB*-amplified), and 10 MTSCC.

Merlin immunohistochemistry

First, the nonneoplastic kidney tissue adjacent to tumor sections was evaluated. Membranous and cytoplasmic expression of merlin was invariably detected in all segments of the renal tubules (convoluted tubules, loop of Henle, collecting ducts) and in the Bowman capsule. In contrast, a much weaker expression was seen in stromal cells and vascular structures.

Next, we evaluated BHP RCC and the RCC subtypes stained for comparison. Almost all BHP RCC (12/13 tumors, 92%) demonstrated complete absence / loss of merlin expression (**Figure 2**), whereas 1 tumor was considered equivocal (case #11). The latter was a BHP-RCC from a prior series arising in a kidney with an adrenal-renal fusion. Although merlin expression was mostly lost in the BHP-RCC (**Supplementary figure**), there were foci (~10% of the tumor volume) with weak cytoplasmic positivity for

the marker. In contrast, all cases of papillary RCC (18/18, 100%) (**Figure 3A, 3B**), *TFE3*-rearranged RCC (10/10 100%) (**Figure 3C, 3D**), *TFEB*-altered RCC (15/15 100%) (**Figure 3E-3H**), and most MTSCC (7/10, 70%) tumors showed retained merlin expression. All tumors with retained merlin expression demonstrated membranous and/or cytoplasmic staining for this marker. Interestingly, a subset of *TFEB*-altered RCC tumors (4/15, 27%) also demonstrated nuclear merlin expression (**Figure 3G-3H**). All comparator tumors exhibited merlin expression of at least moderate intensity in >10% of the tumor cells, with multifocal to diffuse staining that was significantly stronger than that seen in adjacent internal control tissues in most tumors. In this study, merlin IHC (with loss of expression) was ~92% sensitive and ~94% specific to distinguish between BHP RCC and the main RCC subtypes included in its differential diagnosis. These results indicate that loss of merlin expression is a reliable surrogate for detection of the *NF2* alterations in BHP-RCC.

Discussion

The classification of renal tumors has significantly evolved since the International Society of Urological Pathology Vancouver Classification of Renal Neoplasia was published in 2013. (11) Currently, the classification of several well-established and emerging entities incorporates clinicopathologic and genomic features. Moreover, molecular analysis of RCC with distinct histopathologic features has identified novel tumor types with defined biological drivers that could be amenable to targeted treatment. However, once features of a distinct entity are discovered via molecular techniques, often morphologic and IHC surrogates can reach a strong diagnosis without

the need for advanced testing. BHP RCC is an emerging entity with ~26 tumors reported in the literature, largely as case series (7-9) and an individual case report.(10) BHP RCC is characterized by somewhat distinctive morphologic features and recurrent purportedly somatic *NF2* mutations, frequently accompanied by loss of 22q resulting in biallelic inactivation of the gene. Of note, loss of *NF2* appears to be a driver (rather than a passenger) event in this tumor type, given the absence of other highly recurrent cancer relevant variants. (7-8) Given that a subset of BHP RCC has demonstrated an aggressive clinical behavior with fatal outcomes, it might be important to correctly classify these tumors for diagnostic and investigational purposes. Since BHP RCC was initially defined by the presence of *NF2* mutations, molecular studies are currently needed to render this diagnosis, limiting the identification of new tumors. In this study, our aim was to investigate the diagnostic value of merlin IHC in 13 BHP RCC, including 10 tumors reported in the original descriptions of this entity. (7-8,10)
A summary of previously reported cases with detailed morphology, immunohistochemistry, and molecular test results are provided in **Supplementary Table S1.**

An important morphologic hallmark of BHP RCC described by Argani et al (7) is the biphasic appearance comprised of variable proportions of larger cells, as well as smaller cells surrounding basement membrane material and scattered psammomatous calcifications. This peculiar arrangement of smaller tumor cells clustered around basement membrane material within larger acini often imparts a glomeruloid appearance reminiscent of *TFEB*-rearranged RCC. However, frequent biallelic

inactivation of *NF2* and the absence of *TFEB* rearrangements suggest a different underlying oncogenic mechanism in this provisional entity. BHP RCC can show intratumoral heterogeneity with histological findings suggestive of other subtypes, such as areas of clear cells with variably papillary or tubulopapillary structures or elongated, branching tubular pattern with a myxoid stroma and prominent sclerosis. (7,9). A subset of BHP-RCC demonstrates significant morphologic overlap with papillary RCC, as demonstrated by a recent study in which re-review of tumors originally diagnosed papillary RCC resulted in the reclassification of 1.3% of these tumors (2/154) as BHP-RCC (12). Importantly, *NF2*-driven RCCs that were formerly classified as papillary RCC may have an aggressive clinical behavior and are potentially amenable to systemic treatment with targeted agents (13). Since this entity was first described, additional reports of RCC purportedly driven by *NF2* inactivation suggest that the morphologic spectrum of BHP-RCC may be wider than initially thought (8,14). Hence, other tumors types such as MTSCC and *TFE3*-rearranged RCC are also part of the differential diagnosis.

The immunohistochemical profile of BHP RCC described in the literature is not specific but the tumors are consistently negative for melanocytic markers, such as HMB45, Melan-A, and cathepsin K, which are often used to identify MiTF family-translocation. RCC. (7-10) BHP RCC show positive immunoreactivity for KRT7 and epithelial membrane antigen (EMA). Notably, one previously reported tumor (7) and one new tumor (case #13) demonstrated a characteristic pattern of KRT7 and EMA expression, with KRT7 positivity restricted to the larger cells and EMA positivity restricted to the

smaller cells. TFE3 or TFEB immunohistochemistry and fluorescence in situ hybridization for *TFE3* or *TFEB* rearrangement were negative in all reported BHP RCCs. In a recent interrogation of a large series of molecularly characterized pleural mesotheliomas (n=84), our group validated merlin as a highly sensitive surrogate marker of homozygous (i.e., biallelic) *NF2* inactivation. Hence, we hypothesized that this immunomarker could also be useful to identify *NF2*-deficient tumors within the spectrum of BHP-RCC (3). In the present study, we found consistent loss of merlin protein expression by IHC in 12 or 13 cases of BHP RCCs, with an equivocal result in the remaining tumor (case #11). In the latter, there was only focal and weak cytoplasmic merlin expression in ~10% of the tumor cells. Although expression could be considered lost by comparison to the strong and diffuse expression see in the adjacent adrenal tissue (**Supplementary Figure**), we decided to classify this case as equivocal.

Of note, unlike other IHC markers, merlin targets the purported driver of BHP RCC, likely explaining the relatively good sensitivity and specificity observed in this study. Interestingly, we identified nuclear localization of merlin in a small subset of *TFEB*-rearranged RCC tumors. Alternative splicing of the *NF2* transcript has been well described, resulting in multiple different isoforms of the merlin protein. (15) Chang et al. (16) isolated 8 alternatively spliced isoforms, including the predominant isoforms 1 and 2, which exclude and retain exon 16, respectively. In this study, exclusion of exon 2 resulted in a preferential localization of merlin to the nucleus.(16) Moreover, *NF2* contains a potentially functional nuclear export signal in exon 15, suggesting that the protein might have a biologic function in the nucleus.(16) Therefore, the nuclear

positivity observed in a subset of *TFEB*-altered RCC likely reflects the presence of merlin in the nucleus rather than a mere cross-reaction. A useful characteristic of merlin IHC is that the nonneoplastic renal parenchyma served as an internal control, with all the segments of the renal tubules expressing cytoplasmic and/or membranous staining with apical accentuation along the luminal border. We found that the stromal cells and inflammatory cells often showed positive immunoreactivity as well, with somewhat lower intensity compared to the renal tubules. Selection of a representative paraffin tissue block from the tumor interface to include adjacent renal parenchyma will ensure internal quality control of IHC.

Additionally, two of three tumors in the series of BHP RCC reported by Wang et al. (9) lacked *NF2* mutations. Instead, these two tumors demonstrated *NF2* promoter methylation confirmed by methylation-specific polymerase chain reaction and showed loss of merlin protein expression. Their study demonstrated that an epigenetic silencing is an alternative mechanism of *NF2* inactivation in a subset of BHP RCC lacking *NF2* mutations, highlighting the utility of merlin IHC.

Our findings suggest that loss of merlin expression by IHC may be diagnostically useful in BHP RCC with characteristic (i.e., typical) morphologic features. We propose that merlin can be used as part of an IHC panel including, but not limited to, keratins (e.g., CK7) TFE3, TFEB and melanocytic markers to work up RCCs with fitting morphology. However, tumors with non-typical morphology will likely still require molecular analyses until BHP RCC becomes a more established entity. In this study, merlin IHC was nearly

100% specific to distinguish between BHP RCC and the main tumor types included in its differential diagnosis (papillary RCC, *TFE3*-rearranged RCC*, and TFEB*-altered RCC). These results should be interpreted cautiously given the small size of the present series, which might not have captured rare papillary RCC, *TFE3*-rearranged RCC, and *TFEB*-altered RCC with secondary *NF2* loss. In fact, *NF2* mutations have been previously reported in several types of RCC. (6,17-18) Although it is currently unclear how many of these tumors were BHP RCC (classified as a different tumor type) and how often the *NF2* variants were associated with loss of heterozygosity, secondary biallelic loss of *NF2* may certainly occur in other RCC subtypes.

Merlin protein, encoded by *NF2*, plays a role in regulating cell proliferation and elicits a tumor suppressive effect as an upstream regulator of the Hippo signaling pathway through phosphorylation and degradation of YAP and TAZ. (2,4,19) As expected, merlin loss is associated with increased YAP protein expression. As observed in the study by Chen et al.,(4) unclassified renal cell carcinomas with *NF2* inactivation showed a higher level of expression of YAP/TAZ than tumors without *NF2* loss. Prior studies of BHP RCC demonstrated a variable intensity of nuclear and cytoplasmic immunoreactivity for YAP1, with high background staining in the nonneoplastic kidney. (7) Moreover, other RCC subtypes are known to express high levels of YAP1 protein, further limiting the diagnostic utility of this marker. (20)

Given the recent expansion of the morphologic spectrum of tumors purportedly driven by *NF2* inactivation, the differential diagnosis of BHP RCC might be broader than

initially suspected, including RCC types with aggressive behavior. In the first series of BHP RCC reported by Argani et al.,(7) one of eight patients presented with metastatic disease and had a lethal outcome. In later studies, an aggressive disease course with metastasis was also reported in a significant subset of patients. (8-9) We speculate that, in prior studies, BHP RCC may have been categorized as unclassified RCC or papillary RCC.(8) Therefore, interrogation of archival papillary RCC with unusual morphology and unclassified RCC with merlin IHC may help parse out additional BHP RCC tumors to study their clinical, molecular and pathologic features in further detail.

Finally, renal tumors currently known to harbor NF2 mutations include entities like BHP RCC, MTSCC, collecting duct carcinoma (CDC), RCC type unclassified, and sarcomatoid RCC. (4,21) MTSCC demonstrate unique morphologic, molecular and immunophenotypic features, and unlikely to present as a diagnostic differential for tumor with definitive characteristics of BHP RCC. Likewise, CDCs are considered in the differential, largely manifesting as a tumor with diffusely infiltrating tubular structures, but a less likely possibility given the high proliferative activity. More recently, Wang, et al. (14) reported *NF2* mutations in a subset of renal cell tumors with gonadal sex cord-stromal tumor-like morphology. The presence of Hippo pathway mutations, including NF2, makes such tumors possibly amenable to specific inhibitors in clinical trials targeting this particular pathway (for example, ClinicalTrials.gov Identifier: NCT05228015) (4); it would be interesting to see in the future the outcome and utility of such inhibitors in renal tumors with *NF2* mutations.

In conclusion, BHP-RCC is an entity whose morphologic and biologic spectrum is still evolving. In this context, merlin IHC could be a useful diagnostic tool to identify additional cases and differentiate them from morphologic mimics. Additional studies of larger series are needed to determine the frequency of loss of merlin expression in other RCC subtypes.

Contributions

Concept: Katrina Collins and Andres M. Acosta
Design and coordination: Katrina Collins, Michael Hwang, and Andres M. Acosta
Contribution of cases: All authors
Review and analysis of the data: Katrina Collins, Michael Hwang, and Andres M. Acosta
Manuscript draft and figures: Katrina Collins, Michael Hwang, and Andres M. Acosta
Intellectual contributions and manuscript editing: All authors

References

1. Petrilli AM, Fernández-Valle C. Role of Merlin/NF2 inactivation in tumor biology. *Oncogene.* 2016;35:537-548.
2. Cooper J, Giancotti FG. Molecular insights into NF2/Merlin tumor suppressor function. *FEBS Lett.* 2014;588:2743-2752.
3. Chapel DB, Hornick JL, Barlow J, et al. Clinical and molecular validation of BAP1, MTAP, P53, and Merlin immunohistochemistry in diagnosis of pleural mesothelioma. *Mod Pathol.* 2022.
4. Chen YB, Xu J, Skanderup AJ, et al. Molecular analysis of aggressive renal cell carcinoma with unclassified histology reveals distinct subsets. *Nat Commun.* 2016;7:13131.
5. Mehra R, Vats P, Cieslik M, et al. Biallelic Alteration and Dysregulation of the Hippo Pathway in Mucinous Tubular and Spindle Cell Carcinoma of the Kidney. *Cancer Discov.* 2016;6:1258-1266.
6. Malouf GG, Flippot R, Dong Y, et al. Molecular characterization of sarcomatoid clear cell renal cell carcinoma unveils new candidate oncogenic drivers. *Sci Rep.* 2020;10:701.
7. Argani P, Reuter VE, Eble JN, et al. Biphasic Hyalinizing Psammomatous Renal Cell Carcinoma (BHP RCC): A Distinctive Neoplasm Associated With Somatic NF2 Mutations. *Am J Surg Pathol.* 2020;44:901-916.
8. Paintal A, Tjota MY, Wang P, et al. NF2-mutated Renal Carcinomas Have Common Morphologic Features Which Overlap With Biphasic Hyalinizing Psammomatous Renal Cell Carcinoma: A Comprehensive Study of 14 Cases. *Am J Surg Pathol.* 2022;46:617-627.
9. Wang XT, Xia QY, Fang R, et al. Clinicopathological and molecular characterization of biphasic hyalinizing psammomatous renal cell carcinoma: further support for the newly proposed entity. *Hum Pathol.* 2022;123:102-112.
10. Gopinath A, Mubeen A, Jamal M, et al. Biphasic Hyalinizing Psammomatous Renal Cell Carcinoma: Another Provisional Entity Emerging From the Papillary Renal Cell Carcinoma Pandora's Box. *Int J Surg Pathol.* 2021;29:783-787.
11. Srigley JR, Delahunt B, Eble JN, et al. The International Society of Urological Pathology (ISUP) Vancouver Classification of Renal Neoplasia. *Am J Surg Pathol.* 2013;37:1469-1489.
12. Lobo J, Ohashi R, Amin MB, et al. WHO 2022 landscapre of papillary and chromophobe renal cell carcinoma. *Histopathology.* 2022. Online ahead of print.
13. Yakirevich E, Pavlick DC, Perrino CM, et al. NF2 tumor suprressor gene inactivation in advanced papillary renal cell carcinoma. *Am J Surg Pathol*. 2021;45(5):716-718.
14. Wang G, Amin MB, Grossmann P, et al. Renal cell tumor with sex-cord/gonadoblastoma-like features: analysis of 6 cases. *Virchows Arch.* 2022;480:349-358.
15. Schmucker B, Tang Y, Kressel M. Novel alternatively spliced isoforms of the neurofibromatosis type 2 tumor suppressor are targeted to the nucleus and cytoplasmic granules. *Hum Mol Genet.* 1999;8:1561-1570.

16. Chang LS, Akhmametyeva EM, Wu Y, et al. Multiple transcription initiation sites, alternative splicing, and differential polyadenylation contribute to the complexity of human neurofibromatosis 2 transcripts. *Genomics.* 2002;79:63-76.
17. Linehan WM, Spellman PT, Ricketts CJ, et al. Comprehensive Molecular Characterization of Papillary Renal-Cell Carcinoma. *N Engl J Med.* 2016;374:135-145.
18. Gleeson JP, Nikolovski I, Dinatale R, et al. Comprehensive Molecular Characterization and Response to Therapy in Fumarate Hydratase-Deficient Renal Cell Carcinoma. *Clin Cancer Res.* 2021;27:2910-2919.
19. Zhang N, Bai H, David KK, et al. The Merlin/NF2 tumor suppressor functions through the YAP oncoprotein to regulate tissue homeostasis in mammals. *Dev Cell.* 2010;19:27-38.
20. Rybarczyk A, Klacz J, Wronska A, et al. Overexpression of the YAP1 oncogene in clear cell renal cell carcinoma is associated with poor outcome. *Oncol Rep.* 2017;38:427-439.
21. Pal SK, Choueiri TK, Wang K, et al. Characterization of Clinical Cases of Collecting Duct Carcinoma of the Kidney Assessed by Comprehensive Genomic Profiling. *Eur Urol.* 2016;70:516-521.

Figure legends

Figure 1. BHP RCC. **A, B.** Tumor is circumscribed, unencapsulated neoplasm with solid sheets and cords of infiltrating tumor cells associated with a sclerotic stroma. **C**, Tubulopapillary architecture with cribriform structures clustered around basement membrane material. **D**, Biphasic morphology with large acini with a glomeruloid pattern and clusters of smaller cells associated with basement membrane material.

Figure 2. BHP RCC with corresponding merlin immunostaining. **A, C, G, E**. The tumors show solid and papillary architecture with dual population of larger cells arranged around papillary fronds and small cells clustering around basement membrane–like materials. **B, D, F, H.** The neoplastic cells demonstrate complete loss of immunoreactivity for merlin, whereas the renal tubules and the Bowman capsule within adjacent uninvolved kidney serve as an internal positive control.

Figure 3. Comparator groups with corresponding merlin immunostaining. **A**, Papillary RCC showing pseudostratified ciliated columnar epithelium on papillary cores with abundant and eosinophilic cytoplasm with high nuclear grade. **C**, *TFE3*-rearranged RCC showing nests and papillary structures with clear to slightly eosinophilic cells with voluminous cytoplasm and round nuclei with prominent nucleoli. The neoplastic cells demonstrate diffuse membranous (**B, D**) immunoreactivity for merlin. **E, G**. *TFEB*-rearranged RCC showing a solid to nested architecture with clear to eosinophilic cytoplasm, some with areas of pseudopapillary formations. The neoplastic cells demonstrate diffuse nuclear (**F**) or diffuse membranous (**H**) immunoreactivity for merlin.

Table

Table 1. Clinicopathologic and genetic features of BHP RCC Cases						
Case no.	**Age/Sex**	**Size (cm)**	**Stage**	**Metastasis**	**Molecular analysis/Other**	**Follow-up (mo)**
1	56/M	2.9	pT1aNX		NGS, *NF2* NM_000268.3:c.516+2T>A (splice alteration)**	ANED, 24
2	59/M	3.2	pT1aNX		NGS, *NF2* NM_181832.2:c.1520del (frameshift)**	ANED, 156
3	69/M	4.5	pT1bNX		NGS, *NF2* NM_181832.2:c.955C>T (nonsense)**	LFU, 117
4	88/M	4.0	pT1aNX		NGS, *NF2* NM_181832.2:c.622_623del (frameshift)**	LFU, 10
5	43/M	7.5	pT2aNX	LN	NGS, *NF2* NM_181832.2:c.1142_1149del (frameshift)**	DOC, 8
6	72/F	2.7	pT1aNX	Bone	NGS, *NF2* NM_181832.2:c.1481del (frameshift)**	DOD, 72
7	49/M	3.5	pT3aN1	LN	NGS, *NF2* NM_181832.2:c.854_855del (nonsense)**	ANED, 82
8	70/M	3.6	pT3aN0	Lung	NGS, *NF2* NM_181832.2:c.1285A>T (nonsense)**	ANED, 27
9	67/M	3.7	pT1aNX		NGS, *NF2* NM_181832.2:c.1332dup (frameshift)**	LFU, 10
10	57/M	NA	NA*	LN	NGS, *NF2* NM_181832.2:c.265del	ANED, 18

					(frameshift)**	
11	52/M	1.0	pT1Nx		NGS, *NF2* p.Arg516_Lys523delinsGln **	Unknown
12	60/M	3.5	pT1aNX		Microarray analysis 20.4 Mb loss 1p 97.1 Mb loss of 1p>1q 40 Mb loss of 6p monsomy 9,19, and 22 polysomy 12 and 20	ANED, 20
13	53/F	3	pT1aNX		Not performed	ANED, 6

Abbreviations: ANED, alive with no evidence of disease; DOC, died of other cause; DOD, died of disease; LFU, lost to follow up; LN, lymph node; NA, not available

*Originally diagnosed 2 years prior and treated with ipilimumab/nivolumab with good response; currently progressed and on clinical trial.
**Detailed variants are previously reported (7, 8, 10)

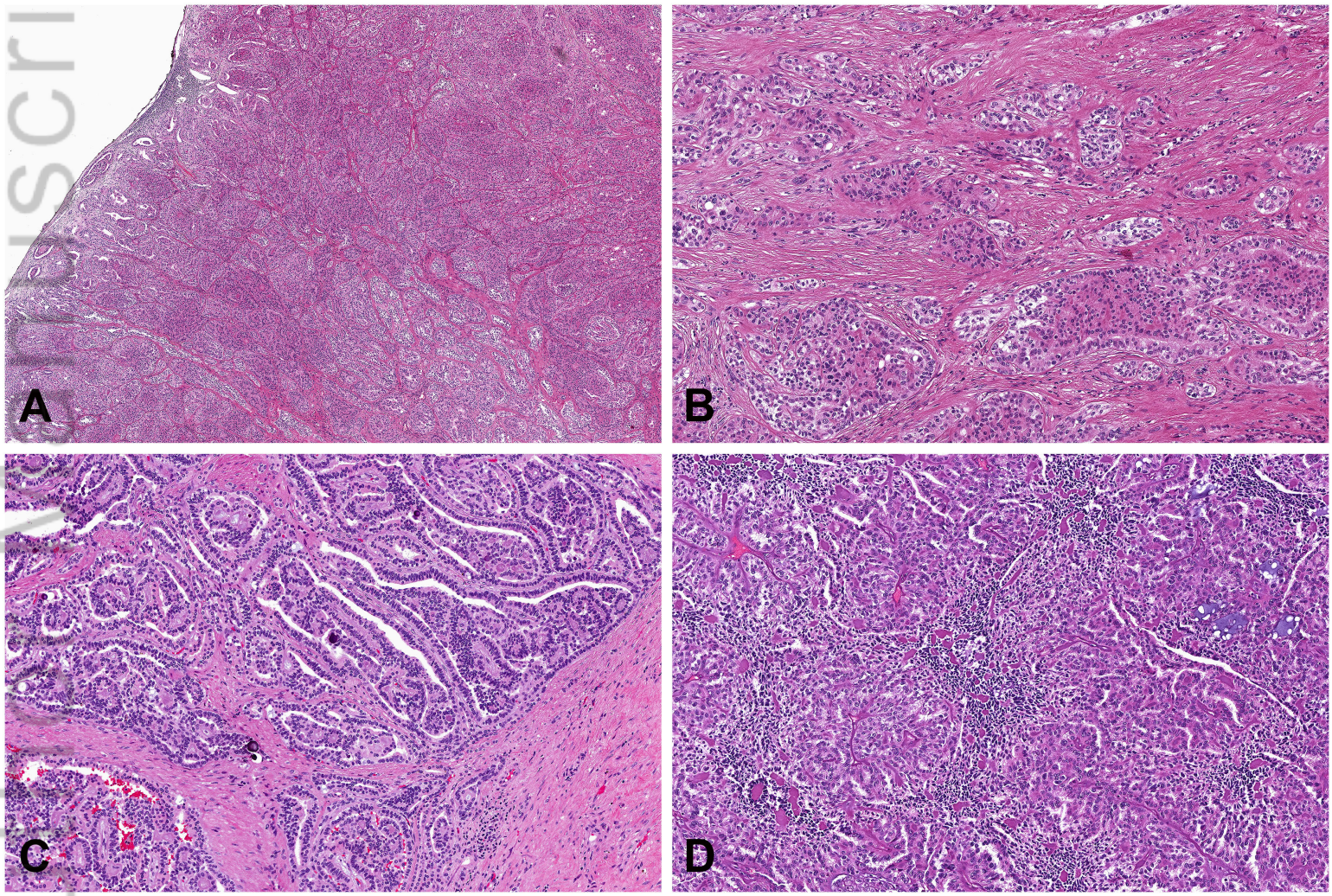

HIS_14731_Figure 1.jpg

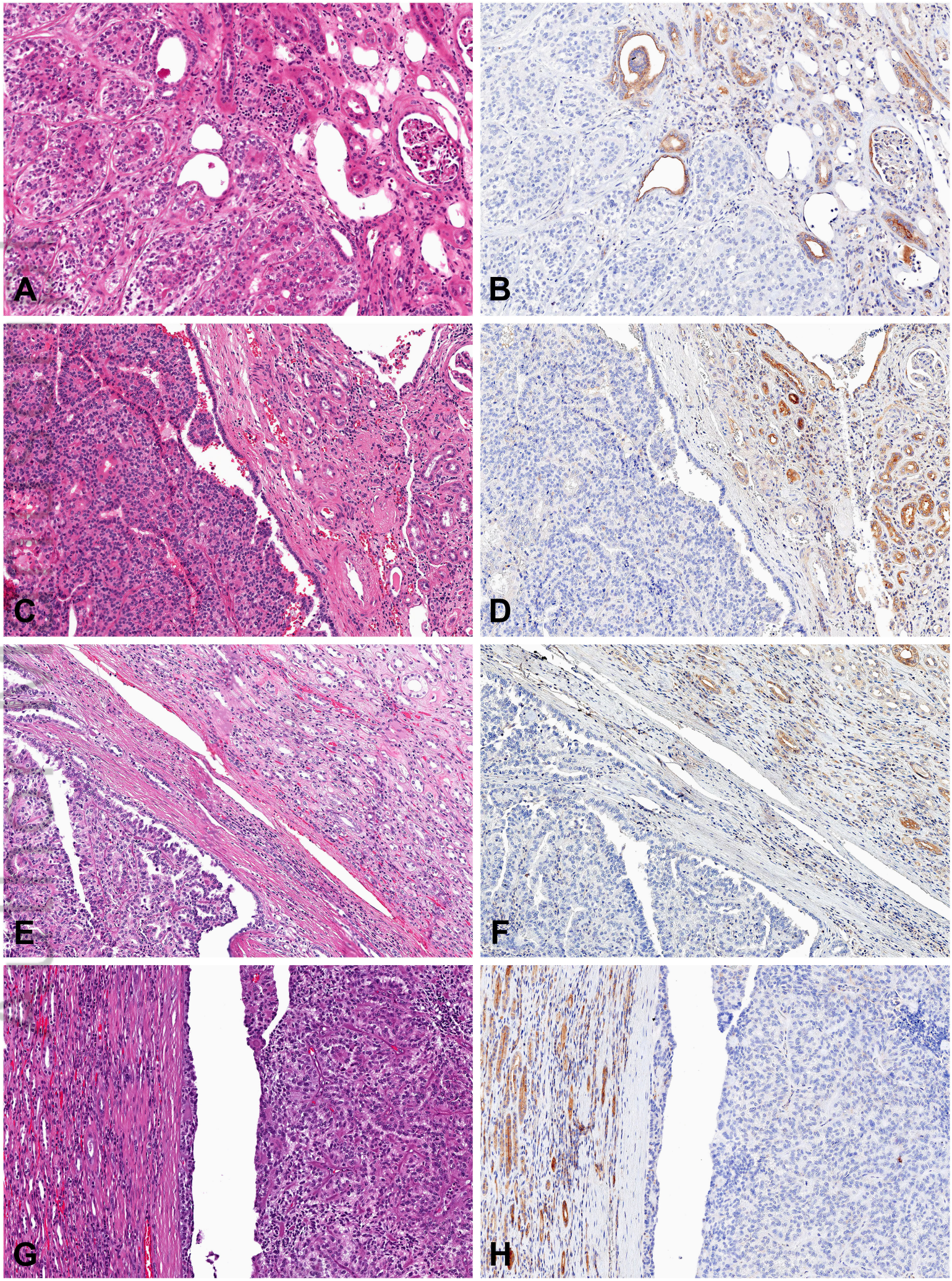

HIS_14731_Figure 2.jpg

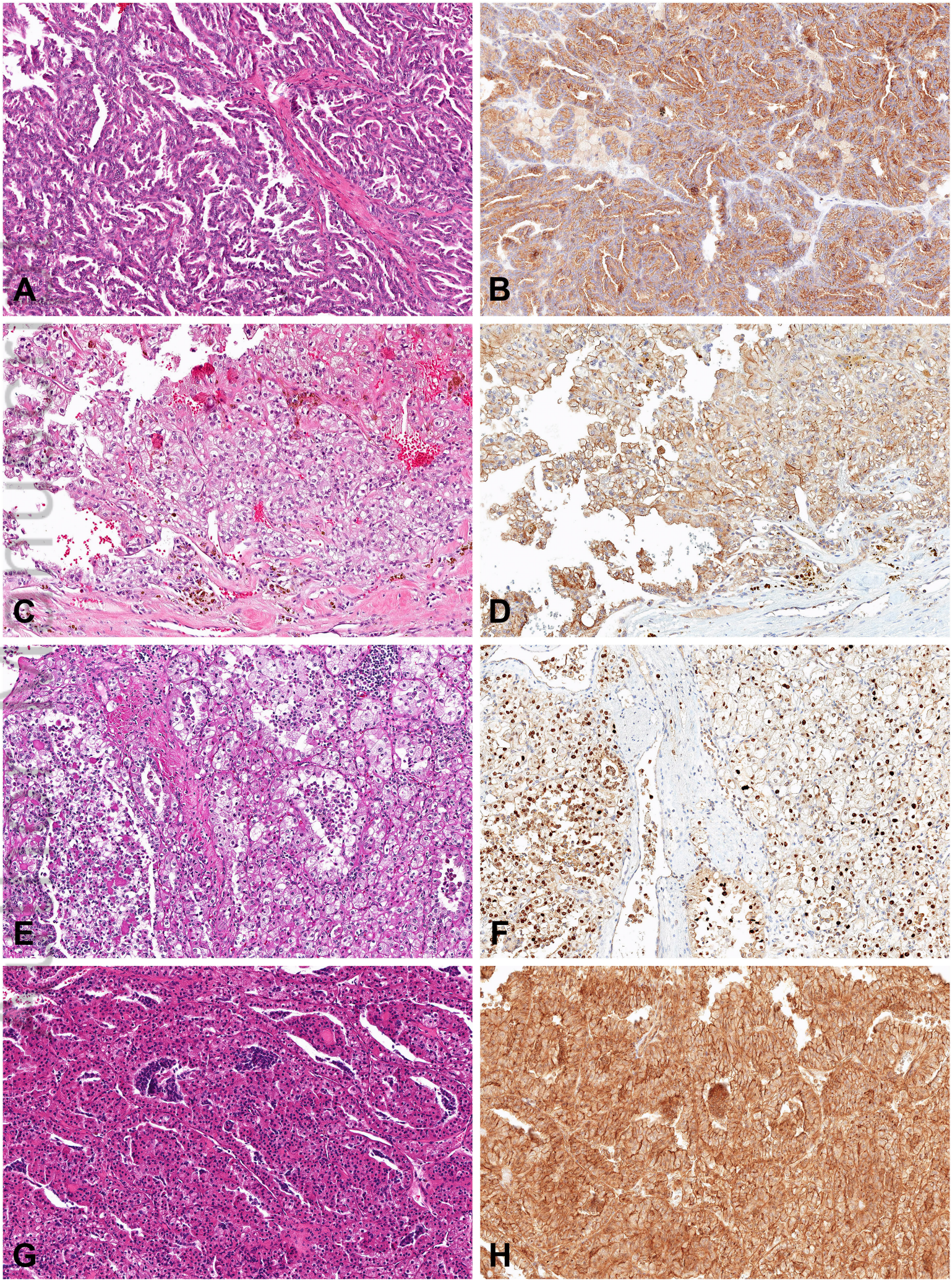

HIS_14731_Figure 3.jpg

Table

Table 1. Clinicopathologic and genetic features of BHP RCC Cases						
Case no.	**Age/Sex**	**Size (cm)**	**Stage**	**Metastasis**	**Molecular analysis/Other**	**Follow-up (mo)**
1	56/M	2.9	pT1aNX		NGS, *NF2* NM_000268.3:c.516+2T>A (splice alteration)**	ANED, 24
2	59/M	3.2	pT1aNX		NGS, *NF2* NM_181832.2:c.1520del (frameshift)**	ANED, 156
3	69/M	4.5	pT1bNX		NGS, *NF2* NM_181832.2:c.955C>T (nonsense)**	LFU, 117
4	88/M	4.0	pT1aNX		NGS, *NF2* NM_181832.2:c.622_623del (frameshift)**	LFU, 10
5	43/M	7.5	pT2aNX	LN	NGS, *NF2* NM_181832.2:c.1142_1149del (frameshift)**	DOC, 8
6	72/F	2.7	pT1aNX	Bone	NGS, *NF2* NM_181832.2:c.1481del (frameshift)**	DOD, 72
7	49/M	3.5	pT3aN1	LN	NGS, *NF2* NM_181832.2:c.854_855del (nonsense)**	ANED, 82
8	70/M	3.6	pT3aN0	Lung	NGS, *NF2* NM_181832.2:c.1285A>T (nonsense)**	ANED, 27
9	67/M	3.7	pT1aNX		NGS, *NF2* NM_181832.2:c.1332dup	LFU, 10

					(frameshift)**	
10	57/M	NA	NA*	LN	NGS, *NF2* NM_181832.2:c.265del (frameshift)**	ANED, 18
11	52/M	1.0	pT1Nx		NGS, *NF2* p.Arg516_Lys523delinsGln **	Unknown
12	60/M	3.5	pT1aNX		Microarray analysis 20.4 Mb loss 1p 97.1 Mb loss of 1p>1q 40 Mb loss of 6p monsomy 9,19, and 22 polysomy 12 and 20	ANED, 20
13	53/F	3	pT1aNX		Not performed	ANED, 6

Abbreviations: ANED, alive with no evidence of disease; DOC, died of other cause; DOD, died of disease; LFU, lost to follow up; LN, lymph node; NA, not available

*Originally diagnosed 2 years prior and treated with ipilimumab/nivolumab with good response; currently progressed and on clinical trial.
**Detailed variants are previously reported (7, 8, 10)